

EXAFS Signatures of Structural Zn at Trace Levels in Layered Minerals

Farid Juillot¹, Guillaume Morin¹, Jean-Louis Hazemann², Olivier Proux²,
Stephanie Belin³, Valerie Briois³, Gordon E. Brown, Jr.^{4,5}, and Georges Calas¹

¹ Institut de Minéralogie et de Physique des Milieux Condensés (IMPMC), UMR CNRS 7590,
Universités Paris 6/7-IPGP, France.

² European Synchrotron Radiation Facility (ESRF), Grenoble, France.

³ Synchrotron SOLEIL, Saint Aubin, France.

⁴ Department of Geological & Environmental Sciences, Stanford University, Stanford, CA, USA.

⁵ Stanford Synchrotron Radiation Laboratory, Menlo Park, CA, USA.

Abstract. Many *in situ* XAFS studies have shown that zinc incorporated in layered minerals is a major form of zinc in Zn-contaminated soils. Quantitative information on the local structural environment(s) and ordering of Zn in these minerals is required to better understand its behavior in soils. In this study, EXAFS spectroscopy was used to assess the structural environment of zinc incorporated at trace levels (40 ppm to 4,000 ppm) within the octahedral sheets of various natural and synthetic layered minerals. Results indicate that EXAFS data analyzed using *ab initio* FEFF calculations (FEFF 8.10) can unambiguously distinguish between zinc incorporation within the octahedral sheet of dioctahedral versus trioctahedral layered minerals and can determine the distribution (random or ordered) of zinc cations within the octahedral sheets of these minerals.

Keywords: Zinc, layered minerals, FEFF, EXAFS

PACS: 78.70.Dm

INTRODUCTION

Numerous studies have emphasized the importance of Zn²⁺ incorporation in layered minerals (clays and LDHs) in controlling the behavior of Zn in contaminated soils [1-5 and references therein]. However, previous *in situ* studies have shown that Zn-bearing layered minerals may exhibit very different EXAFS signals. The reasons for these spectral differences are not well understood as a function of Zn concentration or distribution among crystallographic sites of these minerals. Moreover, questions remain about the partitioning of Zn between these various phases, especially concerning Zn-bearing phyllosilicates, where incorporation in dioctahedral or trioctahedral layers could be related to the origin of Zn (i.e. natural vs. anthropogenic).

This study presents results about the crystal chemistry of Zn²⁺ at trace levels (40 ppm to 4,000 ppm) in octahedral layers of various phyllosilicates with the aim of improving our ability to distinguish different Zn-bearing layered minerals in soils. EXAFS spectra of Zn-bearing synthetic and natural layered minerals were analyzed using FEFF 8.10 and the

results are discussed with respect to Zn concentration and the nature of the octahedral sheets. Particular attention was paid to the distribution of Zn in phyllosilicates with trioctahedral sheets in order to distinguish between ordered vs. randomly distributed Zn²⁺.

METHODS AND MATERIALS

Three synthetic samples (a Zn-rich talc, a Zn-dilute talc, and a Zn-dilute Zn/Al-LDH) and three natural samples (a Zn-dilute biotite, a Zn-dilute illite, and a Zn-dilute kaolinite) were used for this study (Table 1). All were washed 3 to 6 hrs with twice-distilled water acidified to pH 1 with ultra-pure HNO₃ to remove any possible sorbed Zn species before EXAFS analyses. Phase purity of the natural and synthetic studied samples was checked by powder X-ray diffraction (XRD) using CoK α radiation (40 kV, 30 mA).

EXAFS data from these samples were collected at SSRL (Stanford, USA), ESRF (Grenoble, France), and LURE (Orsay, France). Data were recorded at 10 to 20 K in fluorescence or transmission mode, depending on Zn concentration. Energy was calibrated with a Zn

metal foil with the Zn K-edge inflection point chosen at 9659 eV.

TABLE 1. Chemical composition of layered minerals studied as determined by Electron Probe Microanalysis.

Zn-rich talc	$\text{Zn}_3\text{Si}_4\text{O}_{10}(\text{OH})_2\text{nH}_2\text{O}$
Zn-dilute talc	$(\text{Mg}_{2.98}\text{Zn}_{0.02})\text{Si}_4\text{O}_{10}(\text{OH})_2\text{nH}_2\text{O}$
Zn-dilute Zn/Al-LDH	$\text{Zn}_{0.59}\text{Al}_{0.41}(\text{OH})_2(\text{CO}_3)_{0.205}\text{nH}_2\text{O}$
Zn-dilute biotite	$\text{K}_{0.95}\text{Na}_{0.02}(\text{Mg}_{2.21}\text{Fe}_{0.52}\text{Al}_{0.10}\text{Ti}_{0.09}\text{Mn}_{0.02}\text{Zn}_{0.005})(\text{Si}_{2.78-}\text{Al}_{1.22})\text{O}_{10}(\text{OH})_2$
Zn-dilute illite	$\text{K}_{0.73}\text{Ca}_{0.05}\text{Na}_{0.03}\text{Mg}_{0.03}(\text{Al}_{1.28}\text{Fe}_{0.37}\text{Mg}_{0.35}\text{Ti}_{0.04}\text{Zn}_{0.0008})-(\text{Si}_{3.60}\text{Al}_{0.40})\text{O}_{10}(\text{OH})_2$
Zn-dilute kaolinite	$\text{Al}_2\text{Si}_2\text{O}_5(\text{OH})_4$

Fluorescence spectra were analyzed using standard procedures and the XAFS code [6] (see [3] for details). RDFs were obtained by Fourier transformation of the EXAFS using a Kaiser window between 2.5 and 12 Å-1 and a Bessel weight of 2.5 (Fig. 1).

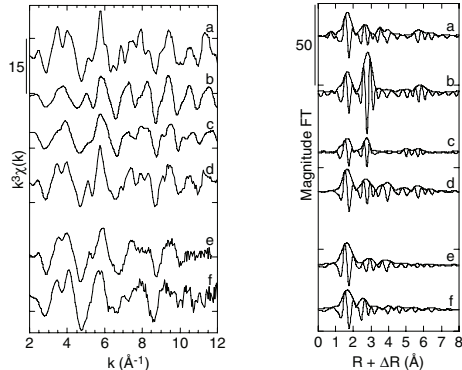


FIGURE 1. EXAFS spectra and RDFs of synthetic and natural layered minerals studied (a: Zn-dilute talc, b: Zn-rich talc, c: Zn-dilute LDH, d: Zn-dilute biotite, e: Zn-dilute illite and f: Zn-dilute kaolinite).

Ab initio Analysis of EXAFS Data

EXAFS spectra were analyzed with FEFF 8.10 [7], using atom clusters 8 Å in radius; the self-consistent potential option was not employed. MS paths with more than 6 legs (NLEG 6) were negligible, and the total number of scattering paths was 500 to 1200, depending on mineral phase. A Debye temperature of 400K and an experimental temperature of 10K were used for all calculations. Energy scales of the FEFF-calculated spectra were shifted +8 eV relative to the Fermi level to fit the experimental EXAFS. Atomic coordinates for FEFF calculations were obtained from the talc [8] and biotite [9] structures. Various $\text{Zn}_x\text{Mg}_{6-x}$

clusters were constructed by replacing Mg^{2+} by Zn^{2+} in the appropriate structure. When necessary, a scaling factor was applied to cell parameters to adjust Zn-neighbor distances. For trioctahedral phyllosilicates, final EXAFS spectra were computed by a linear combination of 1/3 and 2/3 of the spectra calculated with the central Zn at the M1 and M2 sites, respectively. Such a linear combination simulates a random distribution of Zn among the M1 and M2 sites.

RESULTS AND DISCUSSION

Zn Incorporation within Di- vs. Trioctahedral Sheets

Comparison of the RDFs of the experimental Zn EXAFS spectra of the layered minerals considered shows that Zn within dioctahedral vs. trioctahedral sheets yields different feature in the RDFs, especially around 6 Å (uncorrected for phase-shift). This point is well illustrated in Figure 1 where the RDFs of natural and synthetic layered minerals are compared.

This observation agrees with FEFF calculations (not shown) performed on a trioctahedral talc structure, either unchanged or transformed to an M1-vacant dioctahedral structure by removing all M1 atoms [10]. Such calculations show that the RDF peak at ≈ 6 Å arises from a combination of Zn-Mg-Mg and Zn-Mg-Mg-Mg MS focusing paths between collinear edge-sharing $\text{Zn}(\text{O},\text{OH})_6$ and $\text{Mg}(\text{O},\text{OH})_6$ octahedra. In dioctahedral sheets, M1 vacancies inhibit such MS and this peak does not appear in the RDFs.

Effect of Zn Concentration: Example of Talc

Comparison of EXAFS spectra of Zn-pure and Zn-dilute trioctahedral talc samples shows that the latter exhibits more detailed features, but with lower magnitudes (Fig. 2). FEFF calculations on the talc structure with only the central Mg or all Mg replaced by Zn reproduced the experimental EXAFS of the Zn-dilute and the Zn-pure talc samples, respectively. For the latter a scale factor of 1.015 was applied to the cell parameters of talc [8] to account for the slight difference in ionic radius between Zn^{2+} and Mg^{2+} .

RDFs can also be used to distinguish between high and low Zn concentrations in the vicinity of the central Zn atom (Fig. 2). In the case of phyllosilicates, the second peak in the RDFs (2.5-3.0 Å, uncorrected for phase shift) is the most sensitive to Zn concentration because of the large contribution of SS paths between adjacent octahedra. These SS paths occur between edge-sharing $\text{Zn}(\text{O},\text{OH})_6$ octahedra and between $\text{Zn}(\text{O},\text{OH})_6$ and $\text{Mg}/\text{Al}(\text{O},\text{OH})_6$ octahedra in the Zn-pure and Zn-dilute talc samples, respectively. Because of the higher backscattering amplitude of Zn compared

to Mg/Al, the larger the number of Zn^{2+} in the octahedral sheets, the larger the magnitude of this peak.

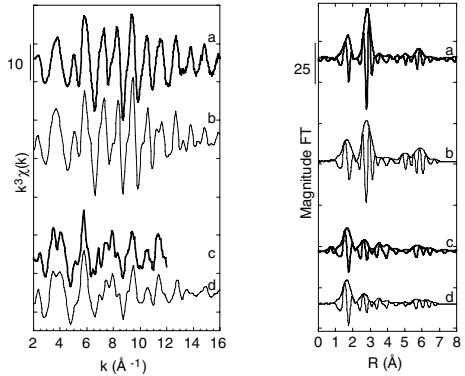


FIGURE 2. Experimental (bold lines) and calculated (thin lines) EXAFS spectra and RDFs of synthetic (a and b) Zn-pure talc and (c and d) Zn-dilute talc.

Zn Distribution in Octahedral Sheets of Dilute Talc

Several FEFF calculations were performed as a function of average 2nd-neighbor environment around Zn for the talc structure (Fig. 3). The first was performed on the non-relaxed talc structure from [8] with only the central Mg replaced by Zn (i.e. a Zn-Mg₆ cluster). The second was done after substitution of an additional Mg among the six within the 2nd-neighbor shell of Zn (i.e. Zn-ZnMg₅). Comparison of these calculations shows that the best match with the experimental EXAFS is obtained from a Zn-Mg₆ cluster, suggesting that no Zn pair occurs in the octahedral sheets of the Zn-dilute talc sample.

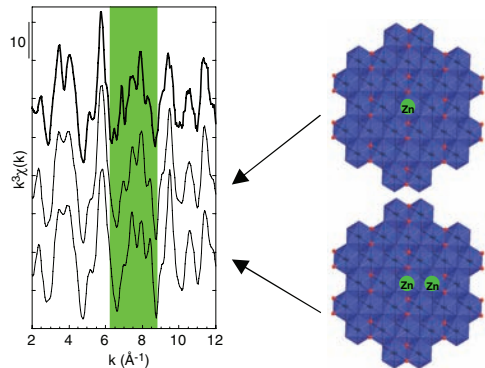


FIGURE 3. Experimental EXAFS spectrum of synthetic Zn-dilute talc (top) compared to calculated ones considering a Zn-Mg₆ (middle) or a Zn-ZnMg₅ (bottom) cluster.

This result compares well with the calculated probability (0.04) of finding adjacent Zn (pairs + trimers + others) in the octahedral sheets of this sample considering a random distribution of Zn using a binomial law. This indicates that 96% of the Zn^{2+} should be surrounded by 6 Mg in the 2nd-neighbor

shell, if Zn is randomly distributed in the trioctahedral sheets of the Zn-dilute talc sample. The good agreement between FEFF results and these probabilities indicates that Zn is randomly distributed in the octahedral sheets of the Zn-dilute talc sample.

The same approach was used for the natural biotite and showed that the experimental EXAFS is best matched using a Zn-FeMg₅ cluster, indicating that Zn-Fe pairs are dominant within octahedral sheets of the Zn-dilute biotite and that Zn (and Fe) are randomly distributed in the octahedral sheets of the Zn-dilute biotite sample.

CONCLUSIONS

Agreement of experimental and FEFF-calculated EXAFS supports structural models in which Zn^{2+} randomly occupies M1 and M2 sites in trioctahedral sheets of phyllosilicates. FEFF analysis of EXAFS of Zn-dilute layered minerals distinguished Zn in dioctahedral vs. trioctahedral layers and revealed the Zn distribution in octahedral sheets of dilute samples. These results will aid identification of Zn species in soils, which is needed to quantitatively describe the (bio)geochemical cycling of Zn at Earth's surface.

ACKNOWLEDGMENTS

This work was supported by the cooperative CNRS-NSF program involving U. Paris VI-VII and Stanford University (grants CNRS-INT-5914 and NSF-INT-9726528), by the European Commission Framework IV Program Grant ENV4-CT97-0554, and by NSF-EMSI Grant CHE-0431425 (Stanford EMSI).

REFERENCES

1. A. Manceau, *et al.*, *Am. J. Sci.* **300**, 289-343 (2000).
2. A. C. Scheinost, *et al.*, *Environ. Sci. Technol.* **36**, 5021-5028 (2002).
3. F. Juillot, *et al.*, *Am. Min.* **88**, 509-526 (2003).
4. A. Manceau, *et al.*, *Geochim. Cosmochim. Acta* **68**, 2467-2483 (2004).
5. A. Voegelin, *et al.*, *Environ. Sci. Technol.* **39**, 6616-6623 (2005).
6. M. Winterer, *J. de Physique VI*, **7**, C2, 243-245 (1997).
7. A. L. Ankudinov, *et al.*, *Phys. Rev. B* **58**, 7565 (1998).
8. B. Perdikatis and H. Burzlaff, *Z. Krist.* **156**, 177-186 (1981).
9. M. F. Brigatti, *et al.*, *Am. Min.* **76**, 1174-1183 (1991).